

Effects of the westerly wind stress over the Southern Ocean on the abyssal circulation

Mikitoshi Hirabara (e-mail:mhirabar@mri-jma.go.jp), Ichiro Ishikawa, and Hiroshi Ishizaki
(Japan Meteorological Agency / Meteorological Research Institute)

1 Abstract

In order to clarify the process through which the change in the westerly wind stress over the Southern Ocean affect the abyssal circulation, numerical experiments are conducted using idealized single-basin and twin-basin (an idealized Atlantic and Pacific) models with a periodically connected passage under various forcings at the surface. Relationships among the northern sinking meridional overturning cell associated with the North Atlantic Deep Water production (NA-cell), the Antarctic Circumpolar Current (ACC), the buoyancy flux, and the wind stress over the Southern Ocean are investigated.

Enhanced westerly wind stress over the Southern Ocean increases the surface buoyancy gain there under the density restoring boundary condition. It is shown that the buoyancy anomalies excited in the Southern Ocean propagate as baroclinic waves into the northern hemisphere, modify the density field, and increase the buoyancy loss, and enhance NA-cell.

Furthermore, buoyancy anomalies excited in the Southern Ocean and enhanced NA-cell warm the global ocean except the southernmost part, therefore intensify the meridional density gradient in the Southern Ocean, and increase the ACC transport.

2 Model configuration

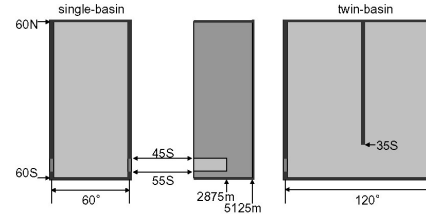


Fig. 1. The topography of the model ocean. (left) Planview of single basin with periodically connected passage ranging from 55S to 45S. (center) Lateral view of basin. It is common to the single basin and the double basin. Flat bottom is 5125m deep while the sill depth of the passage is 2875m. (right) Planview of twin-basin ocean with the same passage as the single-basin ocean. A wall ranging from the northern boundary to 35S partitions the ocean at the mid longitude. Grid spacing: 1×1 degree. Vertically 24 levels.

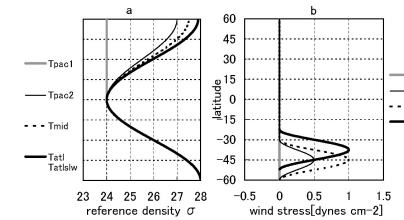


Fig. 2. The profiles of the forcings. (left) Surface reference density σ^* versus latitude. The damping rate of restoring is proportional to 20 days^{-1} for Tpac1, Tpac2, Tmid, and Tat, and 80 days^{-1} for TatSlw. The density in the model is assumed to be a linear function of the temperature. (right) Westerly wind stress versus latitude.

The east basin in the twin-basin is integrated with Tat1 and the west with Tpac1 or Tpac2.

3 Wind stress over the Southern Ocean affects the buoyancy flux in the basin

The model ocean with each forcing is integrated until nearly steady state is obtained.

Using the difference between TatW3 and TatW1 (with identical τ_x at 45S), we examine the wind effect on the change in the buoyancy gain over the Southern Ocean. The anomalous wind driven gyres are shown in Fig. 3 (left). Most of the anomalous northward flows in the subtropical gyre are restricted to the layers near the surface (right top panel), where water is denser for the most part in the TatW3 case than in TatW1 (right bottom) because of the enhanced upwelling in the anomalous subtropical gyre. For an identical reference density σ^* at the surface, the restoring condition give more buoyancy to the TatW3 ocean (center). On the other hand, most of anomalous southward flow, which consists of warm water originating from the lower latitudes, is restricted to the narrow western boundary region, reaching to depth (right top).

As westerly wind stress increases, the pycnocline north of the wind stress maximum is lowered down by the increased Ekman downwelling and become less dense ultimately by the increased buoyancy gain (right bottom).

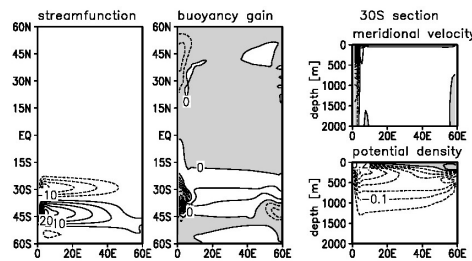


Fig. 3. The difference of the state of TatW3 from TatW1.

(left) Horizontal streamfunction; contour interval 5 Sv. The region of relative high values corresponds to the clockwise circulation around the region. Contour line of zero is not drawn.

(center) Anomalous buoyancy flux at the surface; contour interval $1 \times 10^{11} \text{ g cm}^{-2} \text{ s}^{-1}$. Shading denotes negative values (anomalous buoyancy loss).

(right top) Anomalous meridional velocity in 30S section; contour interval 1 cm s^{-1} . Shading denotes southward anomaly.

(right bottom) Potential density; contour interval $5 \times 10^{-5} \text{ g cm}^{-3}$. Shading denotes the region where TatW3 is denser than TatW1.

The differences in zonal mean potential density between TatW3 and TatW1 is shown in Fig. 4. The subtropical gyre at the latitude band between the westerly wind stress maximum and the northern end of the circumpolar passage in TatW3 become colder than in TatW1 because of the pumping up of the denser subsurface water. The colder water increases the buoyancy gain. The enhanced subtropical gyre warms the pycnocline there, and the warm region spreads to the northern part of the basin and outcrops there, increasing the buoyancy loss at the northern hemisphere. Thus, the wind stress over the Southern Ocean can affect the buoyancy flux not only in the Southern Ocean but also in the northern deep water formation region.

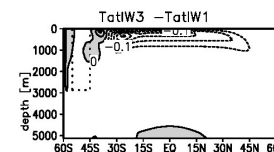


Fig. 4. The difference in zonal mean density between TatW3 and TatW1; contour interval $5 \times 10^{-5} \text{ g cm}^{-3}$. Shading denotes the region where the former case is denser than the latter.

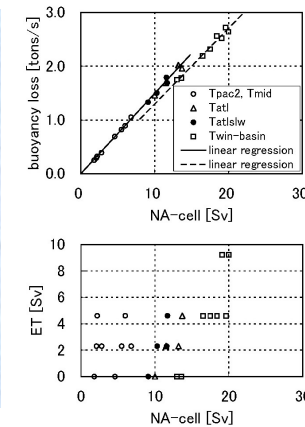


Fig. 5.

(top) The sum of buoyancy loss in the northern hemisphere versus the NA-cell strength. The open circles denote single-basin experiments Tpac2 and Tmid. The triangles denote Tat1 and the closed circles TatSlw experiments. The rectangles denote twin-basin experiments (Tat+Tpac1) and (Tat+Tpac2). The NA-cell strength and the buoyancy loss are integrated in the west basin for twin-basin experiments. The solid line denotes the linear regression for single-basin experiments. The broken line denotes that for twin-basin experiments.

(bottom) The northward Ekman transport at 45S (ET) versus the strength of NA-cell. The marks denote the same as in the top panel.

The top panel of Fig. 5 shows tight relation between the NA-cell strength and the buoyancy loss integrated in (the west basin of) the northern hemisphere.

Enhanced Ekman transport inside and outside of the channel increases the buoyancy gain over the Southern Ocean, warms the pycnocline spreading into the northern part of the (west) basin, increases the buoyancy loss at the sinking region, and enhance NA-cell.

4 Temporal evolution of density anomaly distribution

Here, we look over the temporal changes in the density distribution after W3 forcing is adapted to the (TatI+Tpac2)W0 solution.

We introduce the shear transport (Borowski et al., 2002) streamfunction ψ_{ST} that visualizes the geostrophic overturning on a planview map when the first baroclinic mode is dominant.

$$\psi_{ST} = \frac{g}{\rho_0 f} \int_{-D}^0 \rho' z dz$$

where, g is the gravitational acceleration, f the Coriolis parameter, ρ_0 a constant reference density, D the depth of the ocean, and ρ' the deviation of density from the horizontal mean density.

Closed ψ_{ST} contours around a relative high center correspond to a clockwise circulation in upper layers and an anticlockwise circulation in lower layers. The high center also represent the buoyancy anomalies near there.

Figure 6 illustrates that vertically integrated buoyancy anomalies (ψ_{ST}) excited in the Southern Ocean propagate into the northern hemisphere as baroclinic waves, and enhance NA-cell in the west basin.

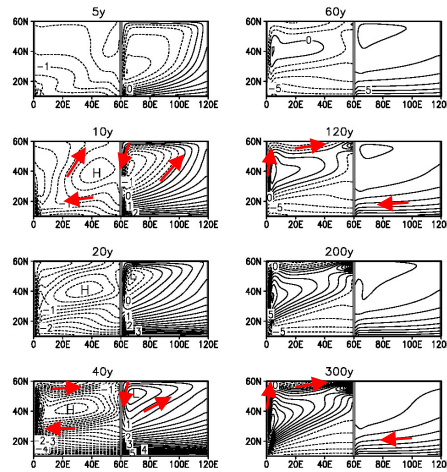


Fig. 6. The anomaly of the shear transport streamfunction (ψ_{ST}) in the twin-basin experiment (TatI+Tpac2) after W3 forcing is adapted on the final state of the (TatI+Tpac2)W0 experiment. Solid contours denote positive values, dashed negatives. Vectors indicate the directions of the anomalous geostrophic flows in the upper layers.

(left) from 5th year (top) to 40th year (bottom); contour interval 0.2 Sv. (right) from 60th (top) to 300th year (bottom); contour interval 1.0 Sv.

The temporal evolution of zonal mean density field and NA-cell is illustrated in Fig. 7. After two years of integration with wind stress, subsurface water to the north of the westerly wind maximum become less dense and that south of the maximum become denser (top panels).

After ten years with wind stress, the region of less dense (by $5 \times 10^{-5} \text{ g cm}^{-3}$) water intrudes into the northern mid-latitudes in the west basin. NA-cell then starts growing (middle panels).

After 100 years of integration, the whole ocean is warmed up, except for the southernmost part and the surface region just to the north of the circumpolar channel. The developed NA-cell is also seen (bottom panels). The buoyancy anomalies excited by the wind stress in the Southern Ocean spread into the northern part of the west basin, reaching to the depth, and strengthen NA-cell.

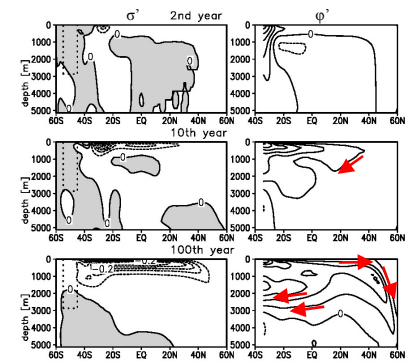


Fig. 7.

(left) The changes in the zonal mean potential density (σ') in the west basin after W3 forcing is adapted on the initial state ((TatI+Tpac2)W0); contour interval $5 \times 10^{-5} \text{ g cm}^{-3}$. Shading denotes the region to be denser than the initial.

(right) the changes in the meridional overturning streamfunction (ψ') in the west basin after the switching on of the wind stress; contour interval 1 Sv.

The states after two years, 10 years and 100 years of integration are shown.

5 The effect on the ACC transport

The ACC transport is set by the meridional density gradient in the Southern Ocean (Fig. 8).

We have already shown that the westerly wind stress over the Southern Ocean modifies the density field of the whole domain.

The wind effect on ACC can be simply understood through the change in the density distribution. The increased westerly wind stress over the Southern Ocean increases the meridional density gradient, and consequently enlarge the ACC transport.

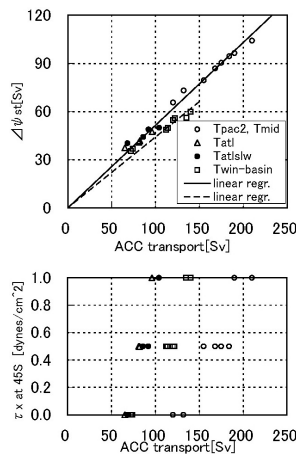


Fig. 8.

(top) The difference between the zonal mean shear transport streamfunction at 45S and that at 55S ($\Delta\psi_{ST}$) against the ACC transport.

(bottom) The zonal component of wind stress (τ_x) at 45S versus the ACC transport.

The marks denote the same as in Fig. 4.

Fig. 9.

The temporal evolution of the ratio of anomaly to the final change. The closed circles denote southward transport of deep water across the equator in the west basin (SF_{EQ}). The rectangles denote the ACC transport.

The temporal evolution of anomalous NA-cell strength and ACC transport after W3 forcing is adapted on the initial state: (TatI+Tpac2)W0.

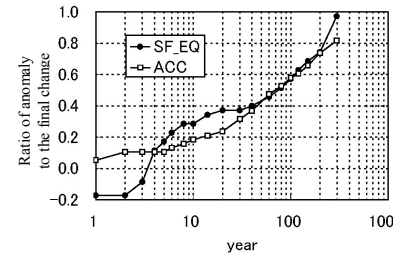


Figure 9 illustrates the temporal evolution of the ACC transport (rectangles) in the same experiment as analyzed above. Southward transport of deep water across the equator in the west basin is also shown (closed circle), which corresponds to the NA-cell strength. In the five years since the wind stress is adapted, anomalous ACC transport reaches only 10% of the final change. It begins to grow after anomalous NA-cell is set up. The warming up of the deep ocean follows the enhancement of NA-cell.

These aspects suggest the importance of the role of anomalous NA-cell for increasing the meridional density gradient that set the ACC transport.

Note that we can attribute the buoyancy anomalies in depths to the results of increased buoyancy gain in the Southern Ocean (Fig. 3).

6 Summary

Increased westerly wind stress over the Southern Ocean excites buoyancy anomalies there. The anomalies propagating into the northern hemisphere change the density distribution, increase the buoyancy loss in the northern part of the west basin, and enhance NA-cell.

The anomalous NA-cell induced by the remote wind stress facilitates warming up of the whole basin, increases the meridional density gradient in the Southern Ocean, and enhances ACC.

7 Reference

Borowski, D., R. Gerdes, and D. Olbers, 2002, Thermohaline and wind forcing of a circumpolar channel with blocked geostrophic contours, *J. Phys. Oceanogr.*, **32**, 2520-2540.

